

Shock wave propagation in vibrofluidized granular materials

Kai Huang,* Guoqing Miao,† Yi Yun, Hua Zhang, and Rongjue Wei

State Key Laboratory of Modern Acoustics and Institute of Acoustics,

Nanjing University, Nanjing 210093, P. R. China

(Dated: June 24, 2021)

Abstract

Shock wave formation and propagation in two-dimensional granular materials under vertical vibration are studied by digital high speed photography. The steepen density and temperature wave fronts form near the plate as granular layer collides with vibrating plate and propagate upward through the layer. The temperature front is always in the transition region between the upward and downward granular flows. The effects of driving parameters and particle number on the shock are also explored.

PACS numbers: 45.70.Mg, 46.40.-f

arXiv:cond-mat/0511692v1 [cond-mat.soft] 29 Nov 2005

*Electronic address: huangkai1996@nju.org.cn

†Electronic address: miaogq@nju.edu.cn

Granular materials are ubiquitous in nature and play an important role in many of our industries and daily lives [1]. Due to their noncohesive, strongly dissipative properties, granular materials behave differently from usual solids, liquids and gases. Under vertical vibrations, as the input energy increases, the state of granular materials changes from solid-like, to liquid-like and gas-like state. The three states and phase transitions between them have been studied experimentally and theoretically [2]. Fluidized granular materials show many interesting phenomena, such as surface pattern [3], oscillon[4], convection [5], size and density segregation [6], cluster [7], heap formation [8] and transport [9]. Recently sound wave propagation attracts much interest because it coexist with most of the above phenomena and is not well understood. It is found that sound in close packed granular materials mainly propagates through force-chains. The speed of sound in sand is approximately the same as that in air and very sensitive to the arrangement of grains [10]. Computer simulations indicate that there exist density and pressure waves in granular materials under vertical vibrations [11]. Recently time-independent shocks in granular flow past an obstacle are observed by experiments and compared with simulation results [12]. Moreover the formation and propagation of shocks in vibrofluidized granular materials have been studied by molecular dynamic simulations and numerical analysis of continuum equations [13]. However experimental study of wave propagations in vibrofluidized granular materials is scarce. In this paper we use high speed photography to explore shock formation and propagation in vertical vibrated bidimensional granular materials.

The experiment is conducted with a rectangular container mounted on the vibrating exciter (Brüel & Kjær 4805), which is controlled by a function generator (type HP 3314A). We use steel spheres with diameter $d = 4 \text{ mm}$ and density $\rho = 7900 \text{ kg/m}^3$. The container is made up of two parallel, $l = 90\text{mm}$ (length) and $h = 280\text{mm}$ (height), glass plates separated by $w = 4.1 \text{ mm}$ vertically adhered in a Plexiglas bracket. The total particle number N , the driving frequency f and the nondimensional acceleration $\Gamma = 4\pi^2 f^2 A/g$ (A is the driving amplitude and g the gravitational acceleration) are used as control parameters. A high speed camera (Redlake MASD MotionScope PCI 2000sc) is used to record the movements of the spheres. A frequency multiplication and phase lock circuit is used to generate external trigger signals for the camera. The acquisition rate is $N_p \times f$ with multiple number $N_p = 25$. Every recorded image is $22d$ (length) $\times 30d$ (height). Image processing technique [14] is used to track the locations of all particles. We use vibrating container as reference frame in image

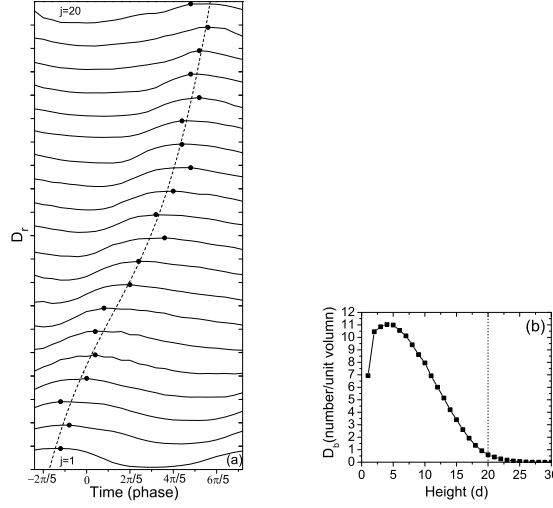


FIG. 1: (a) Time-space profiles of density wave $D_r(j, k)$ from 1st to 20th strips, solid circles peak points of density at each strip, dashed line polynomial fitting of peak values with time; time = 0 corresponds to the time when the plate reaches its maximum height; (b) background density D_b versus height, which is below 1 at height above strip 20 (dotted line). Parameters are $f = 15Hz$, $\Gamma = 5$ and $N = 150$. The height of peak point at each strip is set at 90 percent of total height of that strip.

processing. Every image of grains is divided vertically into a number of strips, each with width of $1d$ and indicated by 1, 2, ... from bottom to top. Assembly average is performed over 600 cycles for granular properties at N_p phase points in each cycle. Granular density $D(jd, k\Delta t)$ is the number of particles in j th strip at time $k\Delta t$, in which $\Delta t = 1/(N_p f)$. For brevity, we omit the units of space and time and use $D(j, k)$ instead of $D(jd, k\Delta t)$ hereafter. Granular temperature is defined by $T(j, k) = \sum_{n=1}^{N_s} \frac{1}{2} |\mathbf{v}_n - \mathbf{v}_b(j, k)|^2 / N_s$, in which N_s is the number of particles in j th strip at time k , \mathbf{v}_n is the velocity vector of the n th particle, and the background velocity $\mathbf{v}_b(j, k) = \sum_{n=1}^{N_s} \mathbf{v}_n / N_s$ is the mean particle velocity in j th strip at the time k averaged over all cycles recorded.

As Γ increases to and beyond 1, granular layer fluidizes from upper to lower parts and the density fluctuations or density wave defined by $D_r(j, k) = D(j, k) - D_b(j)$ (the background number density $D_b(j) = \sum_{k=1}^{N_p} D(j, k) / N_p$) appears in the layer (as shown in Fig. 1(a)). The bottom of the layer reaches its maximum density at time = $-\pi/5$. Fig. 1(a) shows the time-space profile of density wave. The fitting curve of density peaks of all the strips

indicates that the density wave propagates upward with a nonuniform velocity, faster below than above $4th$ strip and is in agreement with the results obtained from molecular dynamic simulations [11]. The wave distorts as it moves upward. It is well known that in ordinary gas the distorted wave will evolve into shock wave as it propagates. The calculation of Mach number Ma indicates that there exists shock wave in our experiment. As a supersonic granular flow encounters an impenetrable plate, velocities of particles (relative to the plate) near the plate abruptly decrease to about zero, but those of undisturbed particles are still unchanged. This results in a normal shock formation near the plate. Then this shock wave leaves plate and propagates upward. We only plot density profiles below $20th$ strip because above that height the number density D_b is too small for accurate statistics (Fig. 1(b)).

In the experiment the shock is identified in a region where the Mach number increases from its minimum (< 1) in the disturbed region to the maximum (> 1) in the undisturbed region. The Mach number is defined by

$$Ma = \left| \frac{v_{bn} - v_p}{c} \right|, \quad (1)$$

where v_{bn} is the vertical component of \mathbf{v}_b , v_p is the velocity of the plate and c is the speed of sound calculated with [13, 15],

$$c = \sqrt{T\chi\left(1 + \chi + \frac{\nu}{\chi} \frac{\partial\chi}{\partial\nu}\right)}, \quad (2)$$

in which $\chi = 1 + 2(1 + e)\nu[1 - (\nu/\nu_{max})^{4\nu_{max}/3}]^{-1}$, e is the restitution coefficient, $\nu(j, k) = D(j, k)\pi d^2/(6lw)$ is the volume fraction and $\nu_{max} = N\pi d^3/(12h_{cm}lw) = 0.57$ is the maximum volume fraction [14]. The height h_{cm} of the center of mass at rest is calculated by

$$h_{cm} = \frac{n_b d}{2N} [(1 - \sqrt{3}/2)n_h + (\sqrt{3}/2)n_h^2] + \frac{n_0 d}{2N} (1 + \sqrt{3}n_h), \quad (3)$$

in which $n_b = l/d - 0.5$ is the average number of particles per strip, $n_h = int(N/n_b)$ is the number of full strip and $n_0 = N - n_h n_b$ is the particle number at the highest strip [14]. We investigate the propagation of the shock by examining the distribution of granular density, temperature and Mach number at four time in one cycle (shown in Fig. 2). The maximum Mach number in the shock and the shock width relative to the mean free path of particles $\zeta = lw/(\sqrt{8\pi}dD)$ [13] as a function of time are drawn in Fig. 3 to show the shock dynamics.

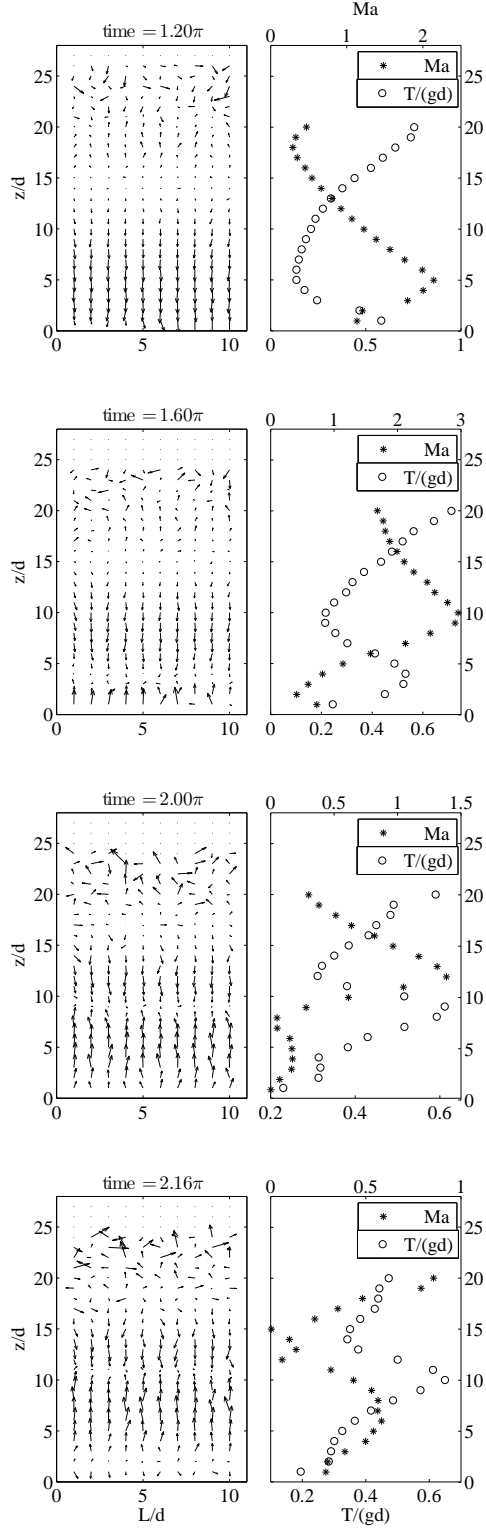


FIG. 2: Velocity field (left column), Mach number Ma (asterisk) and scaled temperature(open circle)(right column) as a function of height(right) at four different times. At time $= \pi$ the plate is at its lowest position. Parameters here are the same as those in Fig.1.

At time = 1.20π , the plate moves upward with $v_p = 0.306m/s$ and begins to collide with the granular layer. Particles at lower strips begin to be compressed by collision. In the mean time most of the particles in the undisturbed region are still falling towards the plate with supersonic speed. This results in the formation of a shock wave. In the shock region the Mach number increases with height and reaches a maximum value 2.73 at the 5th strip. The particle velocities are randomized by collision and the granular temperature decreases with height in this region.

At time = 1.60π , the plate moves upward with $v_p = 0.495m/s$. The granular layer continues to be compressed on the plate, more and more particles come into the compressed region, resulting in the propagation of the shock up through the layer. In the shock region, the Mach number increases with height and reaches its maximum ($Ma = 2.95$) at 10th strip (Fig.3). A temperature peak appears at 3rd strip which is the bottom of shock region and is the transition region between upward and downward granular flows.

At time = 2.00π , the plate reaches its maximum height. The granular layer leaves the plate and flies freely. The shock propagates upward with the maximum Mach number decreasing to 1.39 at the 12th strip. As seen in Fig. 3, the shock width now decreases to its minimum (approximate 1.7 times the mean free path), indicating that the shock is fully developed. The steepen temperature wave front propagates upward to 10th strip.

After time = 2.00π , the plate begins to move downward. The maximum Mach number in the shock region decreases. At time = 2.16π , the shock disappears because the maximum Mach number at strip 13 damps to be less than unity. The temperature wave front continues to propagate upward until disappears in the dilute region of the layer. Then the granular layer is ready for the next collision with the plate.

To investigate how changing Γ and N affect the shock, we perform the experiment with Γ from 5 to 8 and N from 60 to 250. As Γ increases, the velocity of granular layer relative to the plate increases, resulting in the increase of maximum Mach number and the speed of shock. On the other hand, as Γ increases, the average number density decreases (particles expand to more space of the container), and this results in a decrease of the propagating velocity of the wave [16]. As a result the total effects of these two opposite factors make a little change of the velocity of shock with the change of Γ (Fig. 4(a)). As total number of particles increases from 150 to 250 (the layer depth from $7d$ to $11d$) with driving parameters fixed, the average number density increases. As indicated in Fig. 4(b), denser layer collides

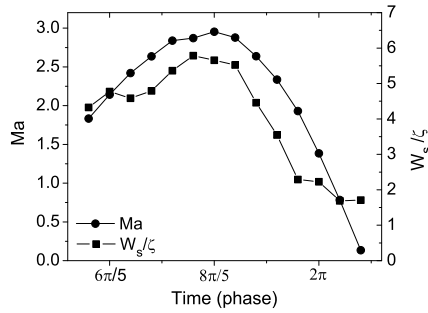


FIG. 3: The peak value of Mach number and shock width W_s/ζ relative to the mean free path ζ as a function of time. The shock begins to form at time= 1.20π and disappear at 2.00π . The shock width decreases to about 1.5 at time= 2.00π , indicating that the shock is fully developed. Parameters here are the same as those in Fig. 1.

with the plate later than more dilute layer. Thus increasing layer depth causes the shock to form later in the cycle and the shock propagates faster through the higher density layer.

In conclusion, we prove the existence of shock wave in vibrofluidized granular materials experimentally. The shock forms as particles collide with vibrating plate and propagates upward with a steepen temperature front in the transition region between upward and downward granular flows. The velocity of shock depends on the velocity of the plate when it collides with granular layer and the number density of granular layer. This is helpful for the understanding of phenomena in vibrofluidized granular materials such as surface instability, convection and energy transfer, etc.

This work was supported by the Special Funds for Major State Basic Research Projects, National Natural Science Foundation of China through Grant No. 10474045 and No. 10074032, and by the Research Fund for the Doctoral Program of Higher Education of China under Grant No. 20040284034.

-
- [1] H. M. Jaeger and S. R. Nagel, Rev. Mod. Phys. **68**, 1259 (1996).
 - [2] A. Goldshtein, M. Shapiro, L. Moldavsky and M. Fichman, J. Fluid Mech. **287**, 349 (1995);
A. Goldshtein and M. Shapiro, J. Fluid Mech. **282**, 75 (1995).
 - [3] F. Melo, P. Umbanhowar and H. L. Swinney, Phys. Rev. Lett. **72**, 172 (1994); F. Melo, P.

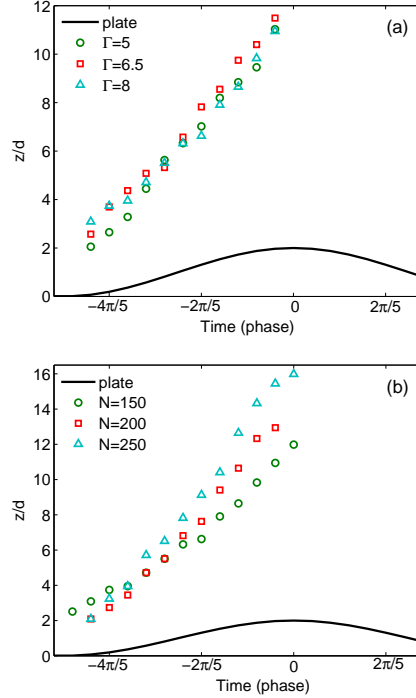


FIG. 4: Shock location as a function of time. with different Γ (a) and N (b). Other parameters are fixed at $f = 20Hz$, $N = 150$ in (a) and $f = 20Hz$, $\Gamma = 8$ in (b). Solid line corresponds to the vibrating plate.

- B. Umbanhowar and H. L. Swinney, Phys. Rev. Lett. **75**, 3838 (1995); E. Clement, L. Vanel, J. Rajchenbach and J. Duran, Phys. Rev. **E 53**, 2972 (1996); S. Luding, E. Clement, J. Rajchenbach and J. Duran, Europhys. Lett. **36**, 274 (1996); C. Bizon, M. D. Shattuck, J. B. Swift, W. D. McCormick and H. L. Swinney, Phys. Rev. Lett **80** 57 (1998).
- [4] P. B. Umbanhowar, F. Melo and H. L. Swinney, Nature **382**, 793 (1996).
- [5] J. B. Knight, E. E. Ehrichs, V. Y. Kuperman, J. K. Flint, H. M. Jaeger and S. R. Nagel, Phys. Rev. **E 54**, 5726 (1996).
- [6] J. B. Knight, H. M. Jaeger and S. R. Nagel, Phys. Rev. Lett. **70**, 3728 (1993); N. Burtally, P. J. King, and M. R. Swift, Science **295**, 1877 (2002).
- [7] S. Miller and S. Luding, Phys. Rev. **E 69**, 031305 (2004).
- [8] M. Faraday, Philos. Trans. R. Soc. London **121**, 299 (1831); P. Evesque and J. Rajchenbach, Phys. Rev. Lett. **62**, 44 (1989).
- [9] K. Huang, G. Q. Miao and R. J. Wei, Int. J. Mod. Phys. **B**, **17**, 4222 (2003).
- [10] C. H. Liu and S. R. Nagel, Phys. Rev. Lett. **68**, 2301 (1992); C. H. Liu and S. R. Nagel, Phys.

- Rev. **B 48**, 15646 (1993).
- [11] K. M. Aoki and T. Akiyama, Phys. Rev. **E 52**, 3288 (1995).
- [12] E. C. Rericha, C. Bizon, M. D. Shattuck and H. L. Swinney, Phys. Rev. Lett. **88**, 041302 (2002).
- [13] J. Bougie, S. J. Moon, J. B. Swift and H. L. Swinney, Phys. Rev. **E 66**, 051301 (2002).
- [14] R. D. Wildman, J. M. Huntley, J.-P. Hansen, D. J. Parker, and D. A. Allen , Phys. Rev. **E 62**, 3826 (2000); S. Warr, G. T. H. Jacques and J. M. Huntley, Powder Technol. **81**, 41 (1994); R.D. Wildman and J.M. Huntley, Powder Technol. **113**, 14 (2000); S. Warr, J. M. Huntley and G. T. H. Jacques, Phys. Rev. **E 52**, 5583 (1995).
- [15] S. B. Savage, J. Fluid Mech. **194**, 457 (1988); P. K. Haff, J. Fluid Mech. **134**, 401 (1983); J. Jenkins and M. Richman, Arch. Ration. Mech. Anal. **87**, 355 (1985); J. T. Jenkins and S. B. Savage, J. Fluid Mech. **130**, 187 (1983).
- [16] S. Harada, S. Takagi and Y. Matsumoto, Phys. Rev. **E 67**, 061305 (2003).